東海大學

資訊工程研究所

碩士論文

指導教授：黃育仁 博士

乳房磁振造影之三維乳腺區域切割

Three-Dimensional Segmentation for Fibroglandular Tissues on Breast MRI

研究生：吳冠澤

中　華　民　國　一　零　七　年　六　月

Three-Dimensional Segmentation for Fibroglandular Tissues on Breast MRI

Advisor

Prof. Yu-Len Huang

Submitted to the Department of Computer Science of

Tunghai University

in partial fulfillment of the requirements for the degree of

Master of Engineering

by

Wu Guan Ze

June 2018

東海大學碩士學位論文考試審定書

東海大學資訊工程學系 研究所

研究生 吳 冠 澤 所提之論文

乳房磁振造影之三維乳腺區域切割

經本委員會審查，符合碩士學位論文標準。

學位考試委員會
召 集 人 ＿＿＿＿＿＿＿＿ 簽章

委 員 ＿＿＿＿＿＿＿＿

＿＿＿＿＿＿＿＿

＿＿＿＿＿＿＿＿

指 導 教 授 ＿＿＿＿＿＿＿＿ 簽章

中華民國 107 年 7 月 2 日

摘要

乳癌是現今婦女最常罹患的癌症，隨著醫學研究的發展與進步，若早期發現並接受治療能夠提高乳癌的治癒率。在醫學影像常用來診斷乳房腫瘤的工具有乳房X光攝影、超音波影像與核磁共振影像，對於電腦輔助分析系統而言，準確的乳腺體積和乳腺密度已被證明可以幫助醫生有效地預測罹癌的風險，在乳房磁振造影(MRI)上進行乳腺輪廓描繪，是一個相當重要的步驟。隨著乳房磁振造影愈來愈廣泛被使用，自動切割乳腺組織變得重要，在臨床上應用很迫切。因此，本研究提出一個乳腺輪廓自動描繪演算法，來輔助醫生判讀乳房磁振造影的乳腺組織資訊。本研究先採用各項擴散異性濾波法進行乳房磁振造影的前處理，以降低影像的雜訊，再調整影像對比度，使得乳腺區域和乳房區域分離並讓邊緣更加明顯，影像切割的主要技術採用三維區域成長法取得乳腺組織，最後再使用型態學的方法將切割的結果進行後處理修補乳腺區域，使得切出來的乳腺組織可以更為精確。本研究總共使用10個病例進行實驗，最後實驗切割出的結果會與醫師手動描繪的乳腺區域進行比較，並計算四個指數(SI、OF、OV、EF)評估相似性。

關鍵字：乳癌，磁振造影，乳腺體積，乳腺密度，影像切割，三維區域成長法

ABSTRACT

Breast cancer is the most common cancer in woman. The development and progress of medical research, if early detection and treatment can improve the cure rate of breast cancer. There are many ways to diagnose breast tumors in medical imaging tools, such as mammography, ultrasonography and magnetic resonance imaging (MRI). In computer aided analysis of MRI, contouring of breast fibroglandular region is an important step. Accurate volume of fibroglandular tissue and breast density should help physicians to effective predict the risk of cancer. As breast MRI becomes more widespread used, a functional automatic method for extracting fibroglandular breast tissue is essential and its clinical application is becoming urgent. This study proposes a robust segmentation method to assist the physician on contouring breast fibroglandular region. The proposed method first utilizes the anisotropic diffusion filtering to reduce the noises and speckle in MRI images. Three-dimensional (3D) region growing method is applied to segment the breast fibroglandular area. Finally, the proposed method obtains the area smoother and correctly though a post processing step. All segmentation methods are three-dimensional, compared to two-dimensional segmentation can be considered more relevance, the results more accurate. This study evaluated total of 10 breast cases and four practical similarity measures (similarity index, overlap fraction, overlap value, and extraction fraction) are used to evaluate the result between the manually determined contours, and the proposed segmentation method.

Keywords: breast cancer, magnetic resonance imaging, breast volume, breast density, image segmentation, three-dimensional region growing

TABLE OF CONTENTS

LIST OF TABLES

LIST OF FIGURES

CHAPTER 1 INTRODUCTION

Among women worldwide, breast cancer is one of the most frequently cancers and the leading cause of cancer death [1, 2]. However, the development and progress of medical research, if early detection and treatment can increase patient survival and mortality benefit. Many studies have shown that a risk of breast cancer in women will increase about 1.8 to 6 times with higher breast density (dense breast tissue) [3]. Breasts are composed of fibroglandular or dense tissue (FGT) and fatty tissue [4]. Dense breast has a lot of fat tissue, but more are breast fibroglandular tissue and connect tissue. Dense type of breast, usually appear in the beginning of menopausal women and women taking hormonal medicine. In these women, many of the results lead to breast fibroglandular tissue, the amount of fibroglandular tissue and connective tissue far more than the breast tissue. Many older women tend to lower the fibroglandular tissue, making their breasts more prone to fatty breast. Due to breast density (BD) was advocated as a risk factor for the development of breast cancer, it is desirable to use it for following the effect of treatment and monitoring subjects at risk [5].

There are many ways to diagnose breast tumors in medical imaging tools, such as mammography, ultrasonography, or magnetic resonance imaging (MRI). The most frequently used tools for detecting breast cancer are mammogram and breast MRI [6]. Before abnormalities become clinically palpable, mammography is the gold standard method in early detection of stage breast cancer. Within screening mammography, full field digital mammography (FFDM) has become more popular and is gradually replacing screen film mammography (SFM) [7]. The advantage of mammography is that it was able to presenting more microcalcifications, which is uncomplicated and not time consuming. Some studies have focused on predict chemotherapeutic effects

with mammography, such as detected tumor size, mammogram density, and texture characteristics of mammograms. However, breast MRI is the most sensitive tool used to detection of breast cancer at an early stage [8]. Breast MRI, a noninvasively and non-radiative medical examination, is used in complement to ultrasound and mammography for cancer diagnosis, staging, and gaining additional knowledge about the tumor biology. MRI also finds usage in screening in high risk patients [9]; nevertheless, the harm of MRI is that patients have to endure more economic load than mammogram.

Along with the development of medical imaging technology, computer aided diagnosis (CAD) system is more extensive used in present society. The use of CAD systems as a 'second reader suggestion' is becoming welcome due to its consistency, reliability and speed [11]. The accuracy of CAD is associated to the location and degree of tumor, the segmentation of the tumor has an immediate impact on the accuracy of medical diagnosis. Contour of breast tumor can be delineated in manual, semi-automatic, or fully automatic approach. Radiologists also could obtain information that is helpful to them by CAD systems, such as the position of breast, the volume of breast, breast density, the volume of fibroglandular, even the tumor information.

In computer vision, image segmentation is the procedure of separating a digital image into multiple paragraphs. The goal of image segmentation is to reduce or transform the signification of the image, making the image easier to understand and analysis [12]. Image segmentation is typically used to locate objects and boundaries (lines, curves, etc.) in images. More exactly, image segmentation is the procedure of allocating a label to every pixel in an image such that pixels with the same label share same visual features.

Medical image segmentation methods would be fundamentally classified as

threshold segmentation method, edge-based segmentation method [13], region-based segmentation method [14] and clustering-based segmentation method. The threshold image segmentation [15] also called histogram thresholding method which depended on the transform of the grayscale or color value to divide contents in an image. Threshold segmentation methods are simple but always acquire the undesirable result when the grayscale distribution is complicated in image. Thresholding methods depend on the change of the grayscale, such as the Otsu's method [16]. The Otsu's method based on the transform of the grayscale and separated image into two parts, the background and objectives. The optimal threshold is computed according to background pixels and objectives pixels.

Segmentation by using edge detection depends on the change of gradient in the image. The classical edge detection methods, such as Canny method [17] and Sobel method [18], were affected effortlessly by the noise and speckle. The region-based segmentation method separated image into many regions. Region growing method, one of the simple region-based image segmentation technique, is based on pre-defined standard for growth into larger regions by grouping pixels or sub-regions. The region growing method needs to select optimal seed points and control the growing the number of times. The main harm of the method is that depended on seed points and growing time.

Clustering-based segmentation methods [19, 20] minimize the intensity distance between every pixel and cluster center, such as K-means clustering method [21]. K-means clustering segmented image into K clusters iteratively, mainly inside the large measures of data to find the most delegate data points. The data is separated into many clusters by repeated iteration until no changes and then the method can create the result of clustering segmentation. However, the K-means clustering data is also sensitive to noise and solitary points. This method must set the count of clusters,

and numerous confidence on the initial value.

Threshold segmentation obtains a good result when the intensity distributions of objects and background pixels are sufficiently different in an image, it is possible to apply a single (global) threshold value to the entire image. Edge-based segmentation utilizes the gradient of the image to determine the edge of the object. Clustering-based segmentation must set the number of clusters and choose a good initial value to classify the pixels of the image. However, the breast fibroglandular is a connected tissue in breast MR images. By using a regional growth method to choose an appropriate seed point, the best breast fibroglandular area would be grown completely, so the region-based segmentation is the best approach in this study.

In order to obtain the better result of segmentation, image pre-processing procedure was applied to promote the image quality. The proposed method utilized the anisotropic diffusion filtering to reduce the noises and speckle in breast MRI. Then three-dimensional (3D) region based method [22, 23] was performed to segment the fibroglandular breast tissue. The 3D region growing method [24] clustered the area by using spatial information in image. The benefit of the method is that performs well with noise, speckle and the disconnected area of the image were not grouped together. Finally, the morphological operators were applied to smooth the edge and fill the hole inside the fibroglandular breast tissue.

Four practical similarity measures between the manually resolute contours and the automatically detected contours were computed for quantitative analysis of the contouring result. This study compared the proposed method with the manually resolute contours. The result of computer simulation showed that the proposed method always achieved the reliable performance.

CHAPTER 2 MATERIALS AND METHODS

2.1 Materials

Breast MRI was performed with the patient in the prone position. Examinations were performed with a 3.0-T commercially available system (Verio®; Siemens AG, Erlangen, Germany) and use of a dedicated16 Channel breast coil. Imaging sequences included a localizing sequence, an axial tse_T1 weighted (3 mm), tse_T2_tirm, pre, during, and post-Gd 3D-FSPGR (1 mm) with fat saturation images, before and five times after rapid bolus injection of 0.1 mmol/L gadobenate dimeglumine (Multihence®; Bracco, s.p.a., Milano, Italy) per kilogram of body weight at a rate of 2 ml/s; followed by a saline flush, acquired at 60 second intervals were obtained. All obtained images were stored on the hard disk and transferred to a personal computer using a DICOM (Digital Imaging and Communications in Medicine) connection for image analysis.

2.2 The Proposed Method

The outline overview of the whole segmentation work-flow is illustrated in Fig. 2.1. The details of each main step are depicted in the following sections.

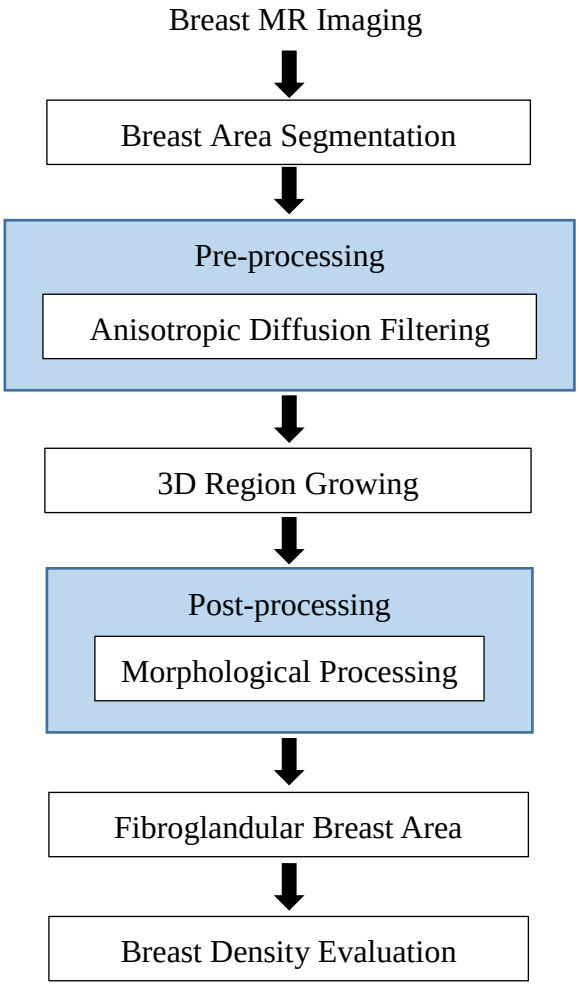

Figure 2.1: Flowchart of the proposed method

2.3 Breast Area Acquirement

During detection of fibroglandular breast tissue in breast MR images, the regions that are negligible such as lungs, heart and thoracic cavity must be removed cautiously to cut down the computation and promote the accuracy of segmentation. The proposed method utilized our previous breast area segmentation (BAS) method [25] to obtain the volume of interest (VOI) on MRI. This automatic method was used to detect contours of breast region on MRI. The BAS method performed a thresholding method and morphological processing to decrease the noises and retain the shape of the breast. Then the projection techniques were performed in the BAS method to distinguish breast region from other tissues.

In this study, the horizontal projection acquired the histogram that calculated by the pixels which value equals to one in the pre-processed image. By this step, the maximum value of projection could be observed, and set as the point of delimitation. By the coordinate of delimitating point, it is easy to define the delimitating line to separate the image into the lower region and the upper region. The green line in Fig. 2.2 is the border between breast and the internal organs. Moreover, the vertical projection was used to separate the breast area and the tissues near the breast. Similar to the horizontal projection, the vertical projection acquired the histogram that counted by the white pixels in the pre-processed image. Then, the breast region would be segmented more precisely. Figure 2.3(a) displays the segmentation after the vertical projection. The red line is the start point of the breast and the blue line is the end point of the breast. Obviously, the rough breast boundary was detected. Figure 2.3(b) shows the preliminary result of the proposed projection segmentation. The contours determined by the method achieved the high similarity to manual sketched contours. Figures 2.4 demonstrates results of the automatic BAS method.

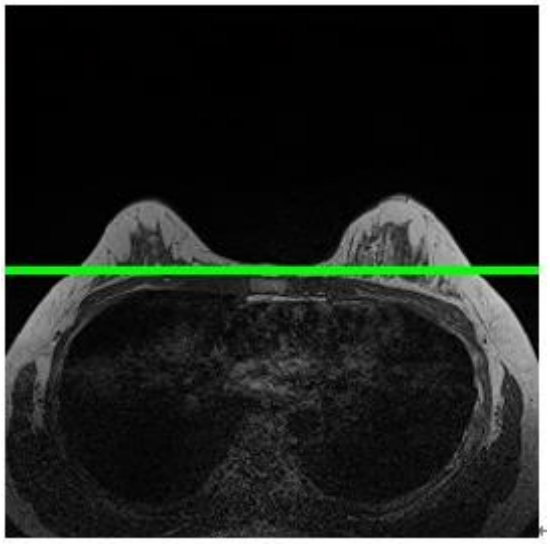

Figure 2.2: Horizontal projection breast segmentation: Segmented breast area

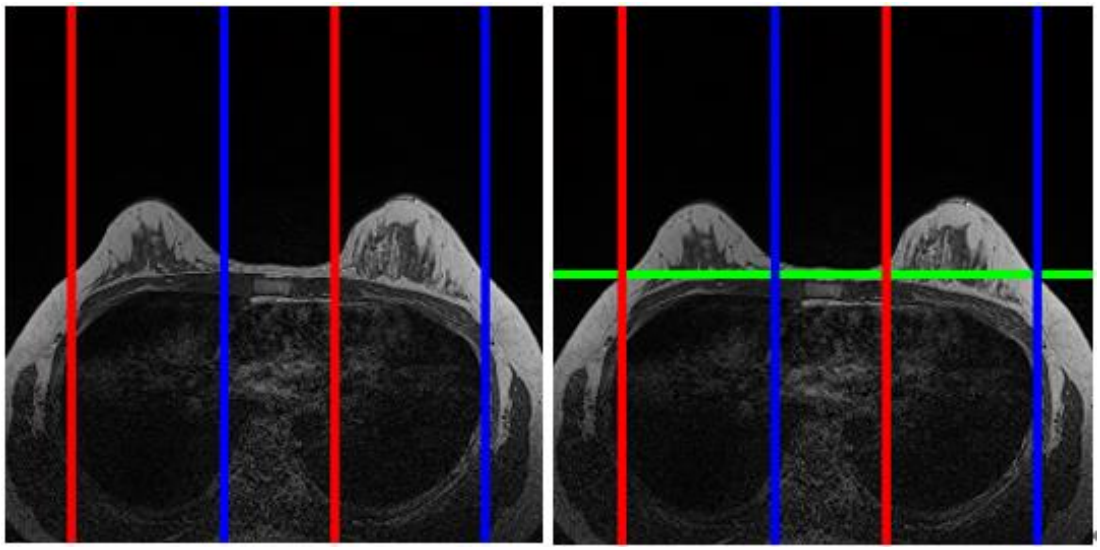

(a) (b)

Figure 2.3: Vertical projection breast segmentation. (a) Segmented breast area, (b) The breast region after horizontal and vertical projection segmentation

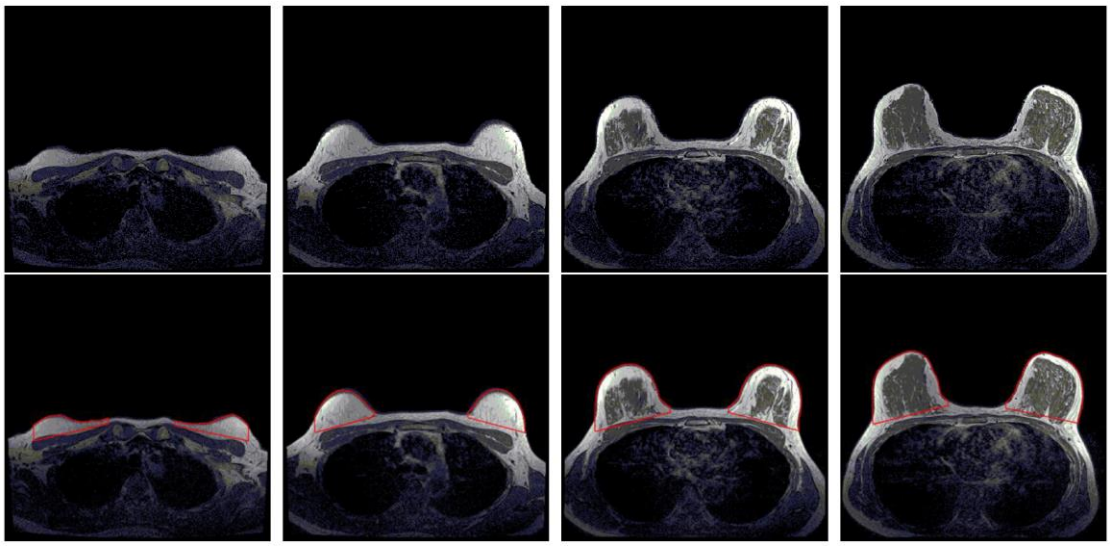

Figure 2.4: The result of the automatic breast segmentation: the upper row images are the original breast MRI and the lower row images show the identified breast areas (red contours)

2.4 Image Pre-processing

Due to breast MR images always include noises, speckles and tissue textures that make segmentation difficult. Therefore, preprocessing is a significant issue before the segmentation. The effective preprocessing method for contouring should aim to

reduce noises and preserve the useful information, such as edge and boundary of the fibroglandular breast tissues.

The anisotropic diffusion method which based on a fractional differential equation is very practical not only in image de-noising but also in preserving the important boundary information. Unlike other filters, such as Gaussian low-pass filter, would acquire a pleased performance on reducing noise but always lose the detail information at the same time. Anisotropic diffusion growled the architecture from the base a Gaussian vague. The method is effective to reduce noise, but not reduce to major part of image.

Formally, let $\Omega \subset R^2$ represent a subset of the plane and $I(\cdot, t)$: $\Omega \rightarrow R$ be gray-level images of a family, the anisotropic diffusion is defined as

$$\frac{\partial I}{\partial t} = \mathrm{div}(c(x,y,t)\nabla I) = \nabla c \cdot \nabla I + c(x,y,t)\Delta I, \tag{2.1}$$

where Δ denotes the Laplacian, ∇ denotes the gradient, div(…) denotes the divergence operator, and c(x, y, t) denotes the diffusion coefficient. The rate of diffusion is controlled by c(x, y, t). It often chosen as a function of the image gradient to reserve the edges of the image. P. Perona et al. proposed the idea of anisotropic diffusion and defined two functions for the diffusion coefficient

$$c(\|\nabla I\|) = e^{-(\|\nabla I\|/K)^2}, \tag{2.2}$$

$$c(\|\nabla I\|) = \frac{1}{1+\left(\frac{\|\nabla I\|}{K}\right)^2}, \tag{2.3}$$

where the constant K controls the sensitivity of edges. The proposed method applied the 3D anisotropic filter to enhance MR images. Figures 2.5 show the de-nosed results by applying the anisotropic diffusion preprocessing method and Gaussian low-pass filter. Figure 2.5(a) is an original MRI slice that includes various contrast levels and noises. The processed images obtained by Gaussian low-pass filtering and the anisotropic diffusion filtering are shown in Figs. 2.5(b)-(c), respectively. Obviously,

the anisotropic diffusion method is superior to Gaussian low-pass filtering in removing noise and preserving edges for the MRI.

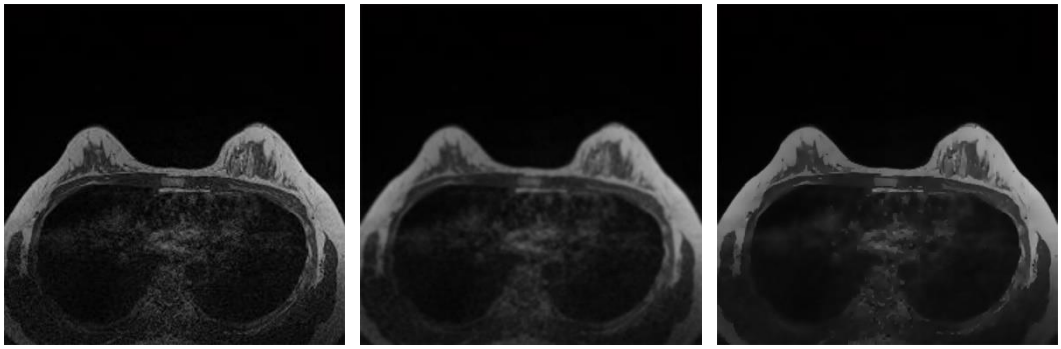

(a) (b) (c)

Figure 2.5: Results of image preprocessing: (a) an original MRI slice, (b) through with Gaussian low-pass filtering, (c) by the anisotropic diffusion method

The idea of threshold segmentation is that the object and background pixels have gray levels grouped into two superior patterns. One evident way to extract the objects from the background is to select a threshold, T, that divides these patterns. Then, any point (x, y) in the image at which f(x, y) > T is called an object point; otherwise, the point is called a background point. In the other words, the segmentation image, g(x, y), is defined as [26]

$$g(x,y) = \begin{cases} 1 & \text{if } f(x,y) > T \\ 0 & \text{if } f(x,y) \leq T \end{cases}, \tag{2.4}$$

when T is a constant applicable over whole image, the procedure given in this equation is consulted to as global threshold. When the value of T changes over an image, we use the term variable threshold. The term local or regional threshold is used sometimes to represent variable threshold in which the value of T at any point (x, y) in an image relies on attributes of a neighborhood of (x, y). If T relies on the spatial coordinates (x, y) themselves, then variable threshold is often consulted to as dynamic or adaptive threshold.

More difficult thresholding problem relating a histogram with three superior

patterns relevant, for example, there are two types of light objects on a dark background. Here, multiple thresholding classifies a point (x, y) as accessary to the background if $f(x,y) \leq T_1$, to one objects class if $T_1 < f(x,y) \leq T_2$, and to the other object class if f (x, y) > T_2.That is, the segmented image is defined as [26]

$$g(x,y) = \begin{cases} a & \text{if } f(x,y) > T_2 \\ b & \text{if } T_1 < f(x,y) \leq T_2 \\ c & \text{if } f(x,y) \leq T_1 \end{cases}, \quad (2.5)$$

where a, b, and c are any three distinct intensity values.

2.5 Fibroglandular Tissue Segmentation

Seeded region growing algorithm [27] is a useful, simple, and sophisticated method for image segmentation. Basically, the concept of 2D and 3D region growing are identical. To decide that the seed surrounding pixels whether to have similar feature with the seed pixel, like gray-scale values, joints and colors. If the surrounding pixels had similar feature with the seed pixel, the surrounding pixel was accepted into the same region and then used as the new kernel. This process continued on every surrounding pixel which was not classified until all pixels of the image were classified. When neighboring pixel and seed pixel gap was less than a predefined property threshold T_p, then the pixel vested in this area, the evolution gone until the region cannot grow outside and formulate a closed area. This study performed the automatic 3D region growing method to separate fibroglandular breast tissue from background.

Let: I(x, y) represent an input image array; S(x, y) represent a seed array which include 1s at the locations of seed points and 0s elsewhere. In gray-level image, 1s represent white pixels, 0s represent black pixels; and Q represent a predicate to be applied at the each location (x, y). Arrays I and S are assumed to be of the same size. A basic region growing algorithms based on 8-connectivity [28] was state as follows:

1. Find all connected components in S(x, y) and corrode each connected component to one pixel; label all such pixels found as 1. All other pixels in *S* are labeled 0.
2. From an image IQ such that, at a pair of coordinates (x, y), let IQ (x, y) if the input image satisfies the given predicate, Q, at those coordinates; otherwise, let IQ(x, y) = 0, using intensity differences as a measure of similarity, thus applied at each location (x, y) is where T is specified threshold.
3. Let *g* be an image shaped by adding to each seed point in s all the 1-vales points in IQ that are 8-connected to that seed point.
4. Label each connected component in *g* with a different region label (e.g., 1, 2, 3, ...). This is the segmented image acquired by region growing.

The center of mass of a system of corpuscles is the point that moves as though: (1) All of the system's mass were centralized there; (2) All outside strength were applied there. Let the mass of the corpuscles are m_1, m_2, …, m_n, which located at x_1, x_2, …, x_n, respectively. If the total mass is M= m_1, m_2, …, m_n, the location of the center of mass (in Fig. 2.6) x_{com} is

$$X_{com} = \frac{1}{M}\sum_{i=1}^{n} m_i x_i. \qquad (2.6)$$

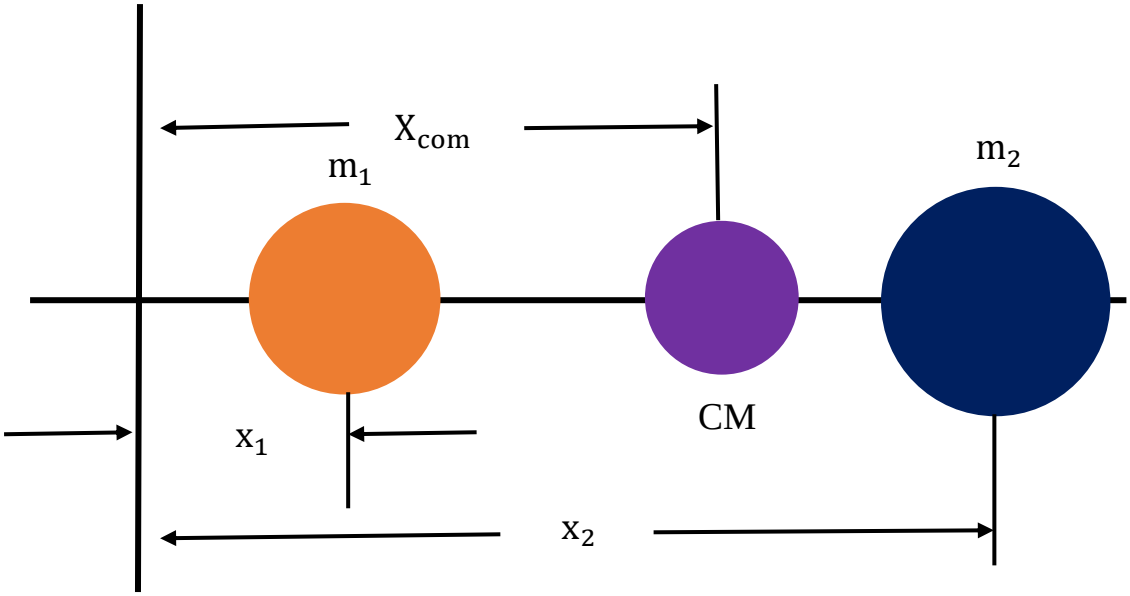

Figure 2.6: Center of mass

The locations of the 3-D center of mass are given by:

$$x_{com} = \frac{1}{M}\sum_{i=1}^{n} m_i x_i \ , \ y_{com} = \frac{1}{M}\sum_{i=1}^{n} m_i y_i \ , \ z_{com} = \frac{1}{M}\sum_{i=1}^{n} m_i z_i. \qquad (2.7)$$

This study utilized the BAS method to generate breast area as VOI. The center voxel of VOI was selected as initial seed point for following region growing. The initial seed point for 3D regional growth was based on by 26 neighbors (26-connectivity) along the seed point to find pixels with similar intensity values (Fig. 2.7), and then the procedure repeated to stop the extension.

1. Utilize selected voxel as the initial seed point
2. Find the local 26- neighborhood voxels of the seed point
3. Absolute difference of intensity between a voxel the seed point, if the intensity of the voxel < T_p, it was assigned into breast fibroglandular region; otherwise, it was considered as the background
4. The whole procedure was repeated until no further changes happen

The 3D region growing method clusters the area using spatial information, it

could perform well to image with noise and speckle and the disconnected area of the image were not clustered together. The proposed method set the center voxel of VOI as an initial seed point due to the largest volume of the breast fibroglandular region always shows in the middle location of breast area.

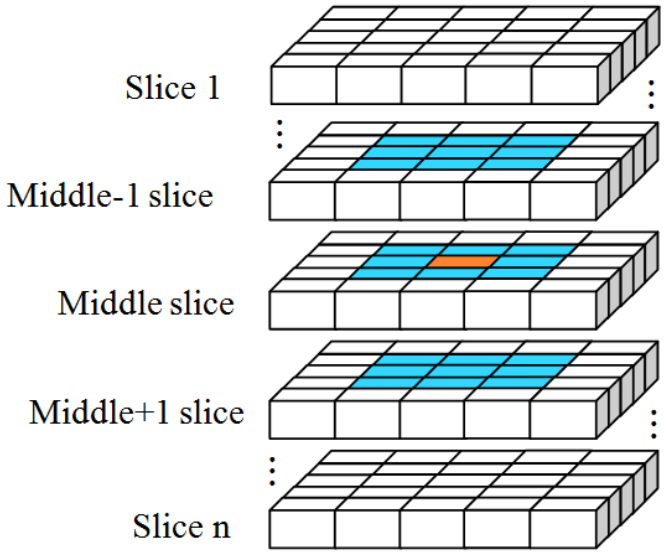

Figure 2.7: Neighbors (the blue voxels) within the 26-connectivity

2.6 Fibroglandular Area Refinement

An extracted breast fibroglandular region was acquired after the segmentation of 3D region growing procedure. However, the procedure might produce excessive tiny bifurcations due to the tissue portion in fibroglandular region possesses a similar intensity sometimes. Thus a post-processing procedure was in need to eliminate the undesired regions of fibroglandular breast tissue. Morphological operators [29], i.e. erosion, dilation, duality, opening, closing, hit-or-miss transformation and fill-hole, were utilized to exclude undesired regions.

- With A and B as sets in z^2 , the dilation of A by B, denoted $A \oplus B$, is defined as

$$A \oplus B = \{z \mid (\widehat{B})_z \cap A \neq \emptyset\}. \quad (2.8)$$

This equation is based on mirroring *B* about its source, and diverting this reflex by z .The dilation of A by B then is the set of all displacements, z, such that $\widehat{B}$ and A overlap by at least one element.

- With A and B as sets in z^2 , the erosion of *A* by *B*, denoted $A \ominus B$, is defined as

$$A \ominus B = \{z \mid (B)_z \subseteq A\}. \quad (2.9)$$

In words, this equation represents that the erosion of A by B is set of all points z such that B, translated by z, is included in A.

- Opening familiarly smoothes the profiles of an object, breaks petty isthmuses, and removes thin protrusions. The opening of set A by structuring element B, denoted $A \circ B$, is defined as

$$A \circ B = (A \ominus B) \oplus B. \quad (2.10)$$

Therefore, the opening A by B is the erosion of A by B, followed by a dilation of the result by B, as shown in Fig. 2.8.

- Closing also tends to smooth sections of profiles but, as opposed to opening, it familiarly fuses petty breaks and long thin gulfs, removes small holes, and fills gaps in the profile. The closing of set A by structuring element B, $A \cdot B$, is defined as

$$A \cdot B = (A \oplus B) \ominus B. \quad (2.11)$$

Which talks that the closing A by B is simply the dilation of A by B, followed by an erosion of the result by B, as shown in Fig. 2.9.

The morphological hit-or-miss transform is a basic tool for shape detection. A hole may be defined as a background region surrounded by a connected border of foreground pixels. Moreover, the post-processing could cause the boundary smoother and fill the holes inter of breast fibroglandular region. Figure 2.10 shows the result of the proposed post-processing procedure.

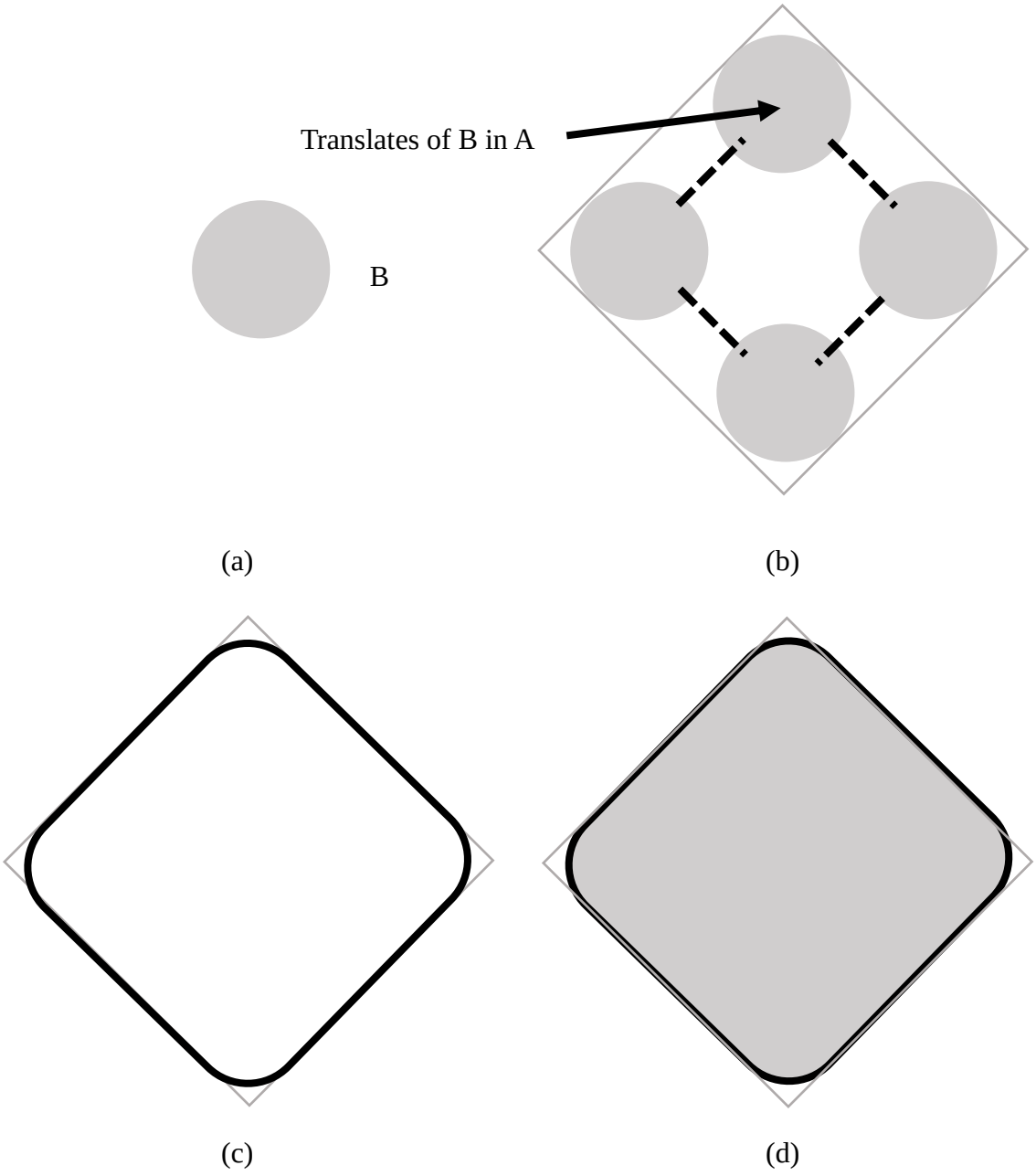

Figure 2.8: (a) Structuring element, (b) structuring element B "rolling" along the inner border of A (the dot represent the origin B), (c) the heavy line is the outer border of the opening and (d) complete opening (shaded)

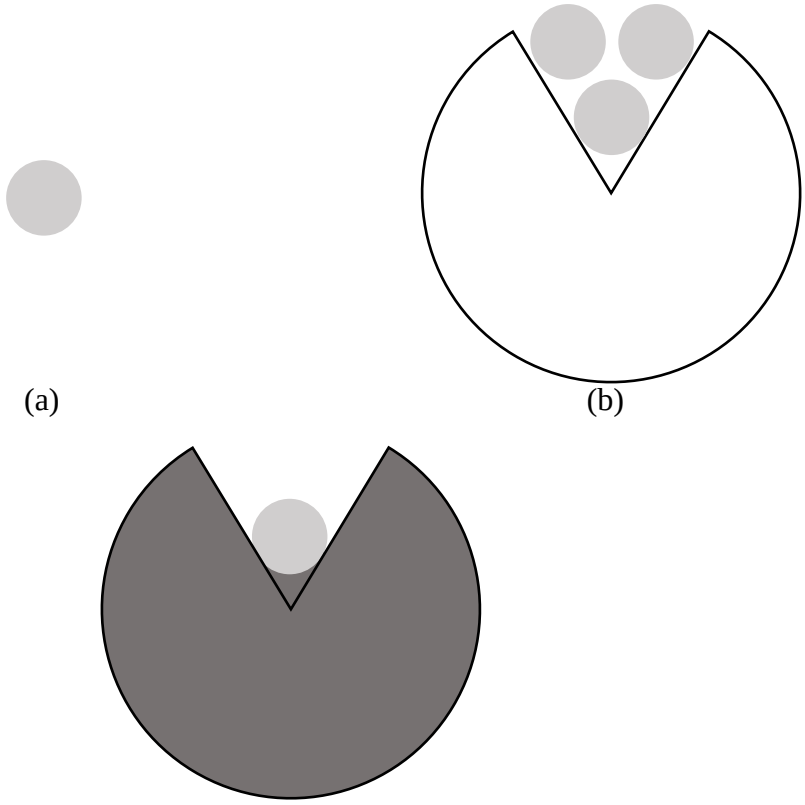

Figure 2.9: (a) Structuring element, (b) structuring element B "rolling" along the outer border of A, then the heavy line is the outer border of the closing and (d) complete closing (shaded)

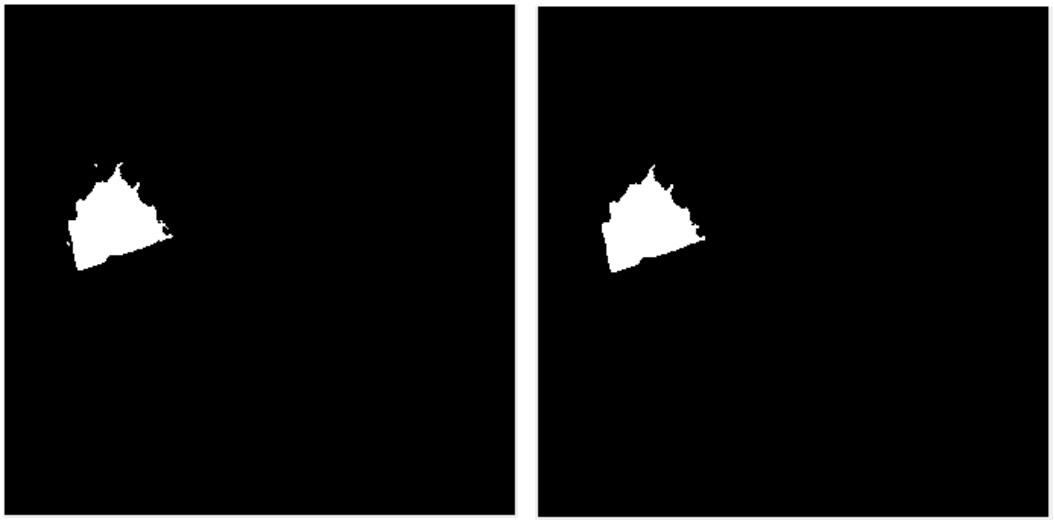

Figure 2.10: Result of the image post-processing: (a) the extracted fibroglandular region and (c) result of the post-processed region

CHAPTER 3 RESULTS

This study totally experimented 10 cases to test the accuracy of the proposed segmentation method. The breast MR images were accumulated by comprehensive Breast Cancer Center of Changhua Christian Hospital, Taiwan. The capturing resolution of breast MR images was 512 × 512 × 60 with 16 bits per pixel. Each monochrome MRI image was quantized into eight bits with 256 gray levels. Field of view (FOV) of the images is 320 mm and the slice thickness is 3 mm. The proposed automatic segmentation method was implemented by Matlab (R2012a, MathWorks Inc., MA). The simulations were performed on a single CPU Intel i7 3.6 GHz personal computer with Microsoft Windows 7 operating system.

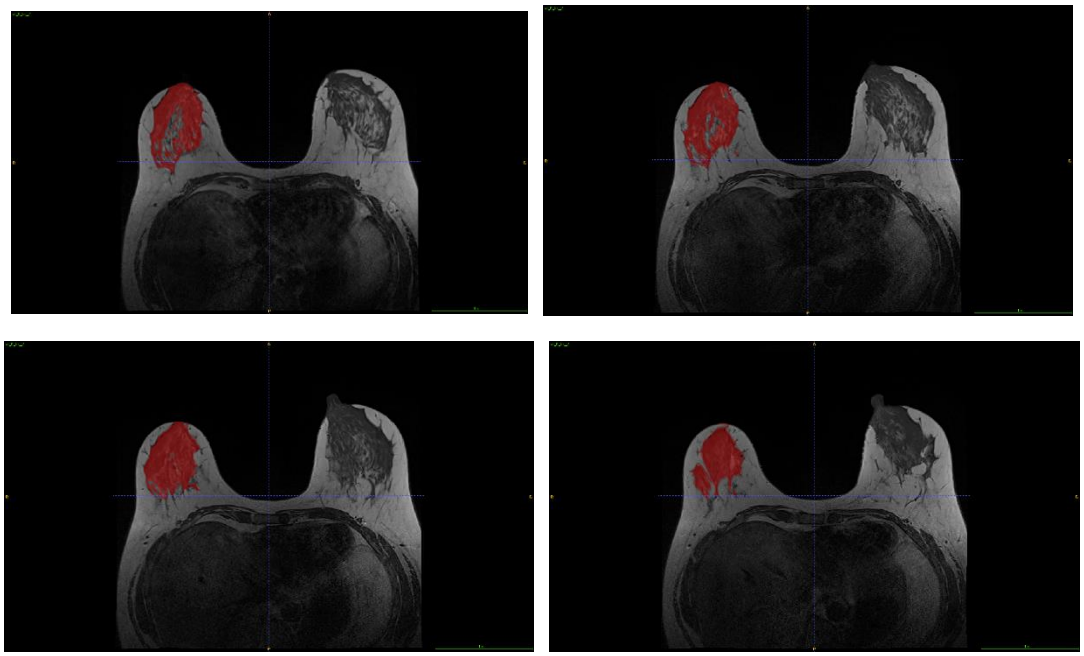

Figure 3.11: Final segmentation results of fibroglandular breast tissues (red regions)

The proposed image preprocessing methods was first performed to reduce noise and preserve detail information. The anisotropic diffusion filtering set the conduction coefficient *kappa* as 70 experimentally. Image segmentation procedure employed 3D region growing method with the intensity threshold T_p as 40 to extract fibroglandular breast tissues. Due to a 3D MRI included numerous image slices, Figs. 3.11

demonstrate the partial segmentation results from a case which extracted the fibroglandular tissue on right breast by using the proposed method. The extracted breast area and fibroglandular tissues were applied to construct and render the 3D demonstration of breast MRI, as shown in Figs. 3.12.

(a)

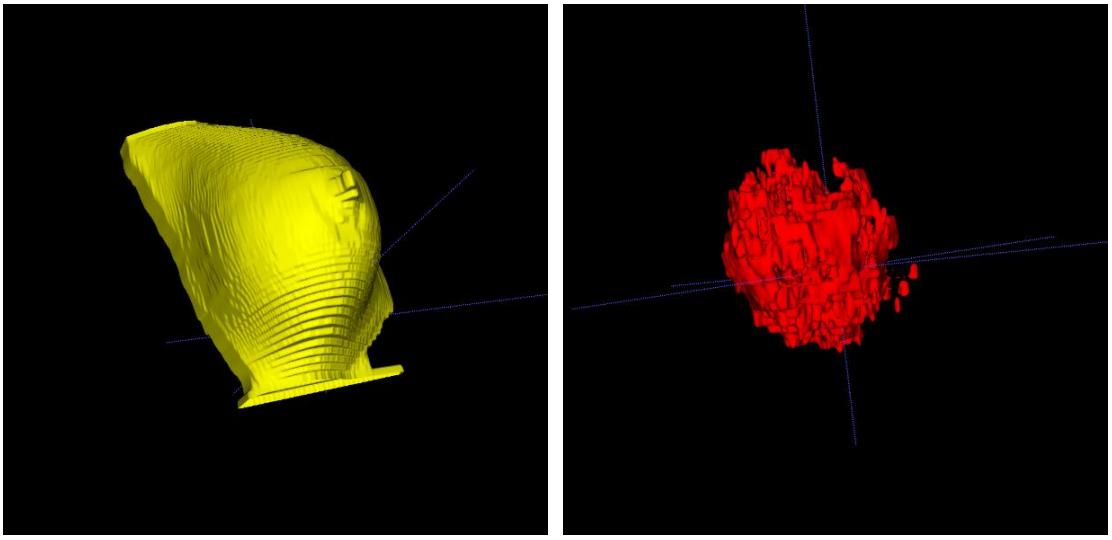

(b) (c)

Figure 3.12: 3D demonstrations (right breast): (a) appearance of the chest, (b) breast area using the BAS method and (c) extracted fibroglandular region using the proposed method

3.1 Breast Density Evaluation

Due to Accurate volume of fibroglandular tissues and breast density have been shown to help physicians to effectively predict the risk of cancer. Breast volume [30] is defined as that analysis on a pixel-by-pixel basis inside the breast (excluding the pectoral muscle). Gland volume is defined as that considers the whole imaged breast contour, including those parts of the breast that were not compressed. Breast density is defined as that the appraised fibroglandular tissue volume by the appraised breast volume to define the volumetric percent of fibroglandular tissue in the breast. Table 3.1 shows the breast volume, gland volume, density values of the 10 cases by using the proposed method.

Table 3.1: Breast volume, gland volume, and breast density values evaluation

Case #	Breast volume(cc)	Gland volume(cc)	Breast density
01	344.28	103.45	0.300
02	526.74	162.53	0.309
03	977.39	197.19	0.202
04	475.43	198.62	0.418
05	229.71	59.11	0.257
06	286.81	66.92	0.233
07	610.61	308.68	0.506
08	835.24	219.39	0.263
09	542.59	223.79	0.412
10	450.86	70.88	0.157

3.2 Evaluation of Contour

Quantitative analysis of four practical similarity measures, the similarity index (SI), overlap fraction (OF), over value (OV), and extra fraction (EF), between the manually resulted contours and the automatically resulted contours comparison. REF stands for the results sketched by the physician manually, and SEG represents the region of breast fibroglandular described by our automatic segmentation method. SI is the similar degree between REF and SEG. The overlap area includes the area of the proposed method and manual sketching by physician, extra area means the false positive area and missing area means false negatives area. Figure 13 illustrates the relationship between the REF and SEG. The SI, OF, OV and EF are defined as

$$SI = \frac{2 * (REF \cap SEG)}{REF + SEG}, \tag{3.1}$$

$$OF = \frac{REF \cap SEG}{REF}, \tag{3.2}$$

$$OV = \frac{REF \cap SEG}{REF \cup SEG}, \tag{3.3}$$

$$EF = \frac{\overline{REF} \cap SEG}{REF}, \tag{3.4}$$

when SI, OF, OV approach to 1, and EF approach to 0, it indicates that the breast fibroglandular area segmented by our method is similar to the result that delineated by physician. The overlap represents the area of the intersection of the reference and the automated segmentation. Table 3.2 shows the four similarity measures of all cases.

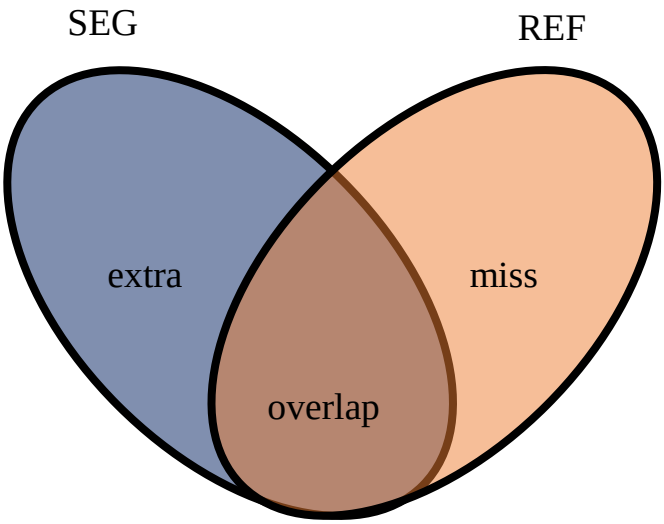

Figure 3.13: The relationship between the tumor segmentation by SEG (segmented by the proposed method) and REF (manually delineated by an experienced physician)

Table 3.2: The four similarity measures of all cases

Case #	SI	OF	OV	EF
2	0.8544	0.8249	0.7458	0.1061
4	0.8047	0.7777	0.6733	0.1551
7	0.8667	0.8789	0.7647	0.1493
8	0.8135	0.8430	0.6857	0.2295

SI: similarity index; OF: over fraction; OV: over value; EF: extra fraction

The segmentation result of proposed method is shown on Figures 3.14-3.17. Figures 3.14(a) to 3.17(a) show Original MRI image. Figures 3.14(b) to 3.17(b) show Region growing result. Figures 3.14(c) to 3.17(c) show post-processed result. Figures 3.14(d) to 3.17(d) show the gland area which sketched manually by physician.

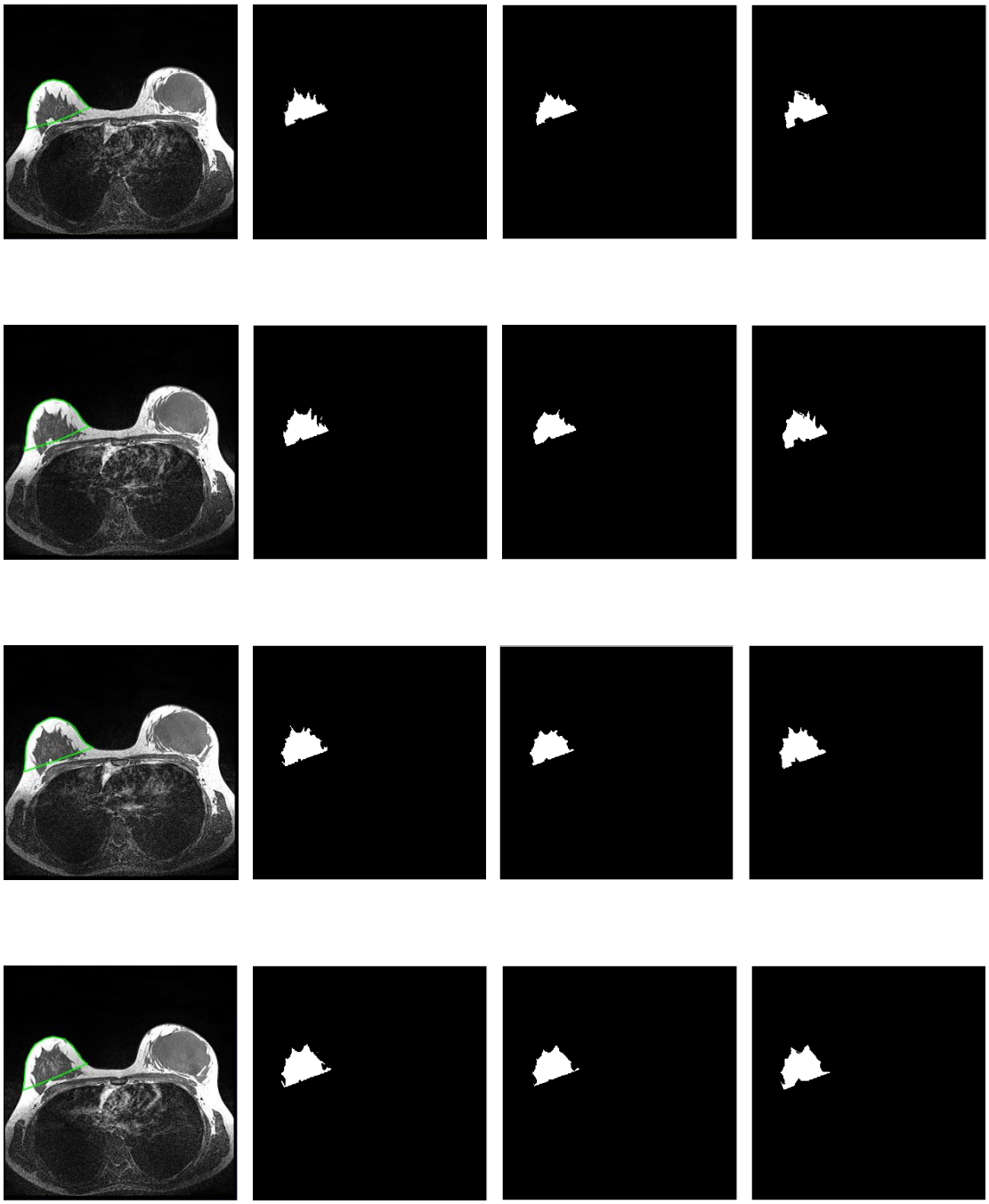

(a) (b) (c) (d)

Figure 3.14: The result of case 2 of proposed method (60 slices per case). (a) Original MRI image (green line is breast area), (b) region growing result, (c) post-processed result, (d) manual gland area by physician

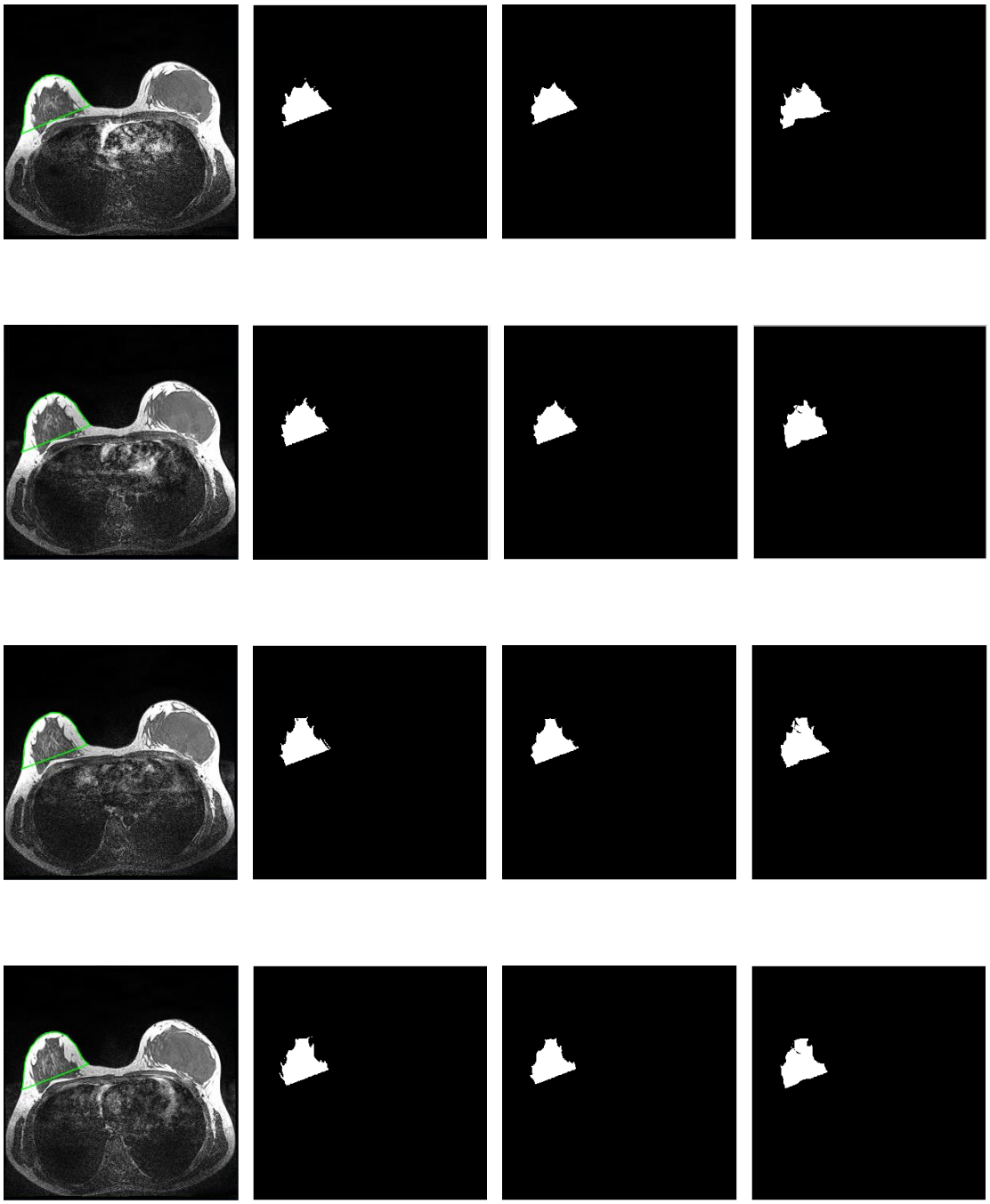

(a) (b) (c) (d)

Figure 3.14: The result of case 2 of proposed method (60 slices per case). (a) Original MRI image (green line is breast area), (b) region growing result, (c) post-processed result, (d) manual gland area by physician (Continued)

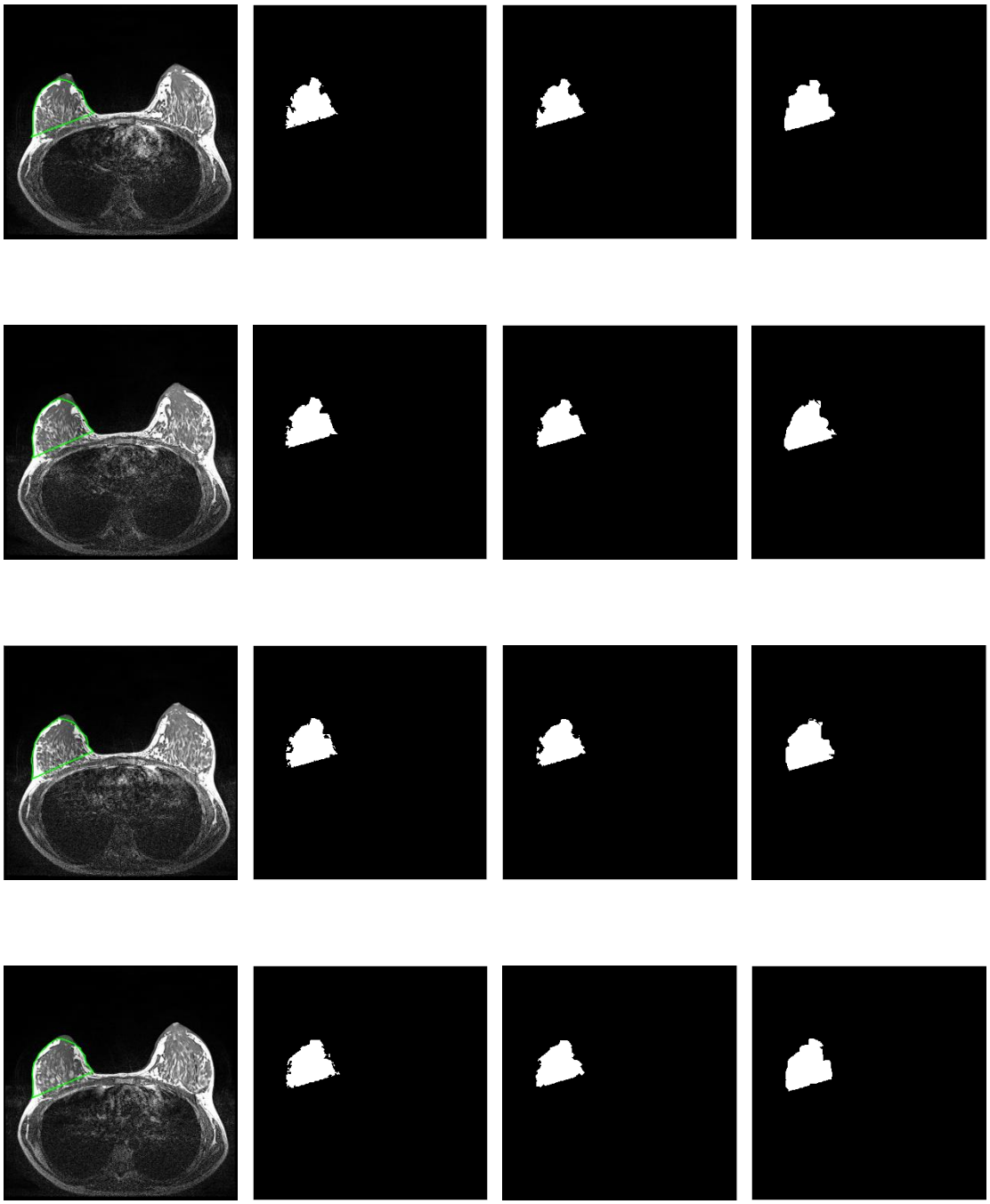

(a) (b) (c) (d)

Figure 3.15: The result of case 4 of proposed method (60 slices per case). (a) Original MRI image (green line is breast area), (b) region growing result, (c) post-processed result, (d) manual gland area by physician

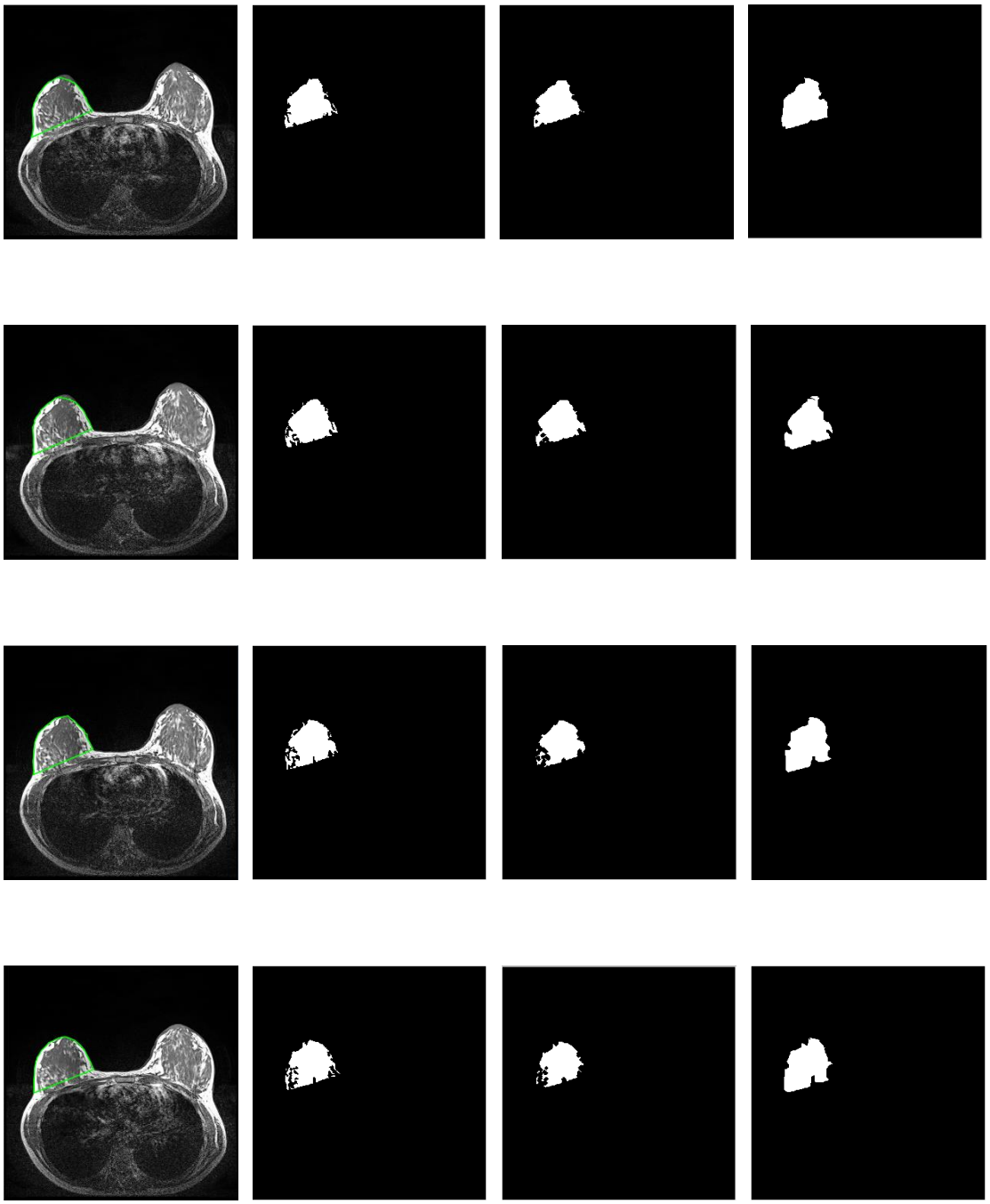

(a) (b) (c) (d)

Figure 3.15: The result of case 4 of proposed method (60 slices per case). (a) Original MRI image (green line is breast area), (b) region growing result, (c) post-processed result, (d) manual gland area by physician (Continued)

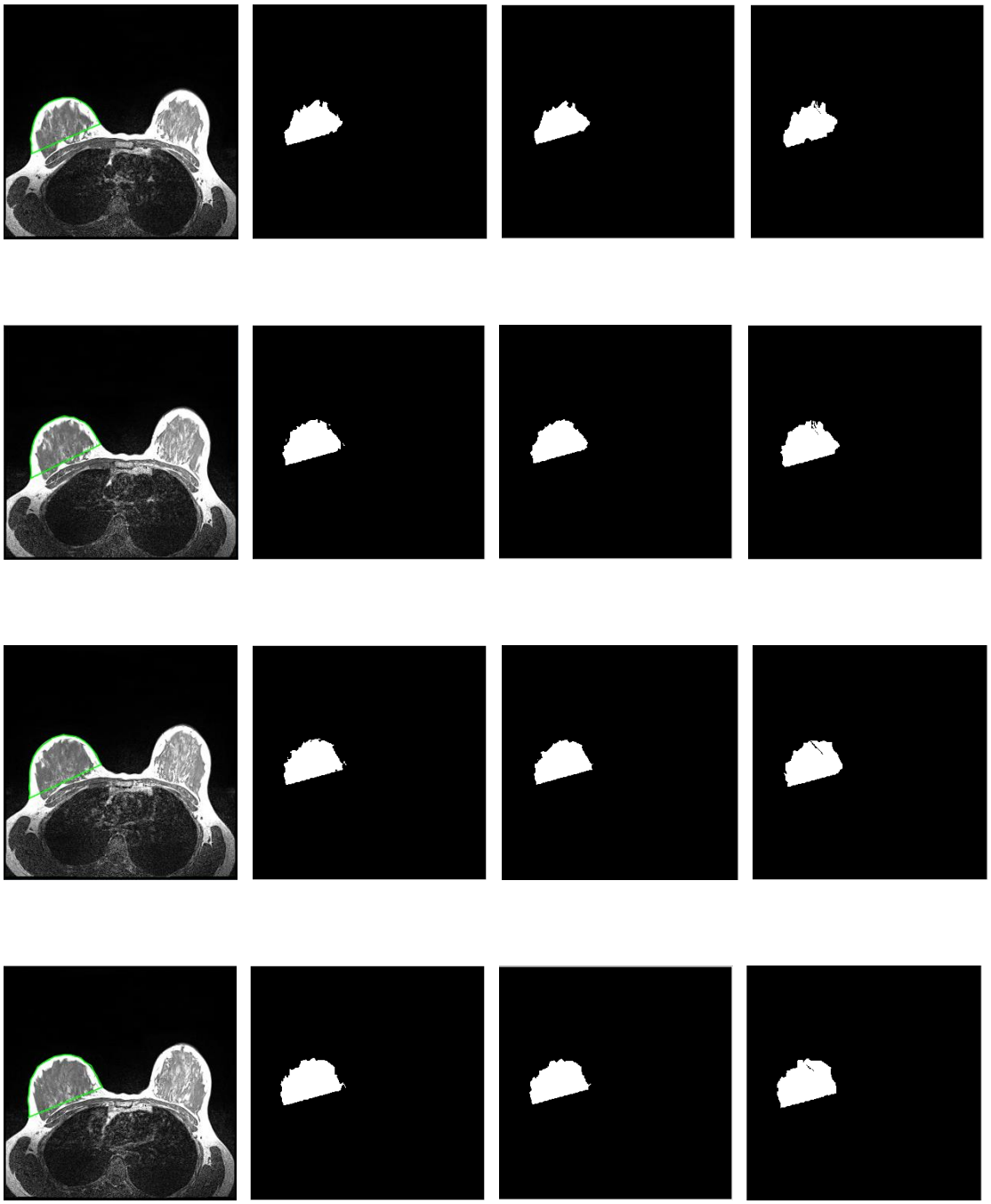

(a) (b) (c) (d)

Figure 3.16: The result of case 7 of proposed method (60 slices per case). (a) Original MRI image (green line is breast area), (b) region growing result, (c) post-processed result, (d) manual gland area by physician

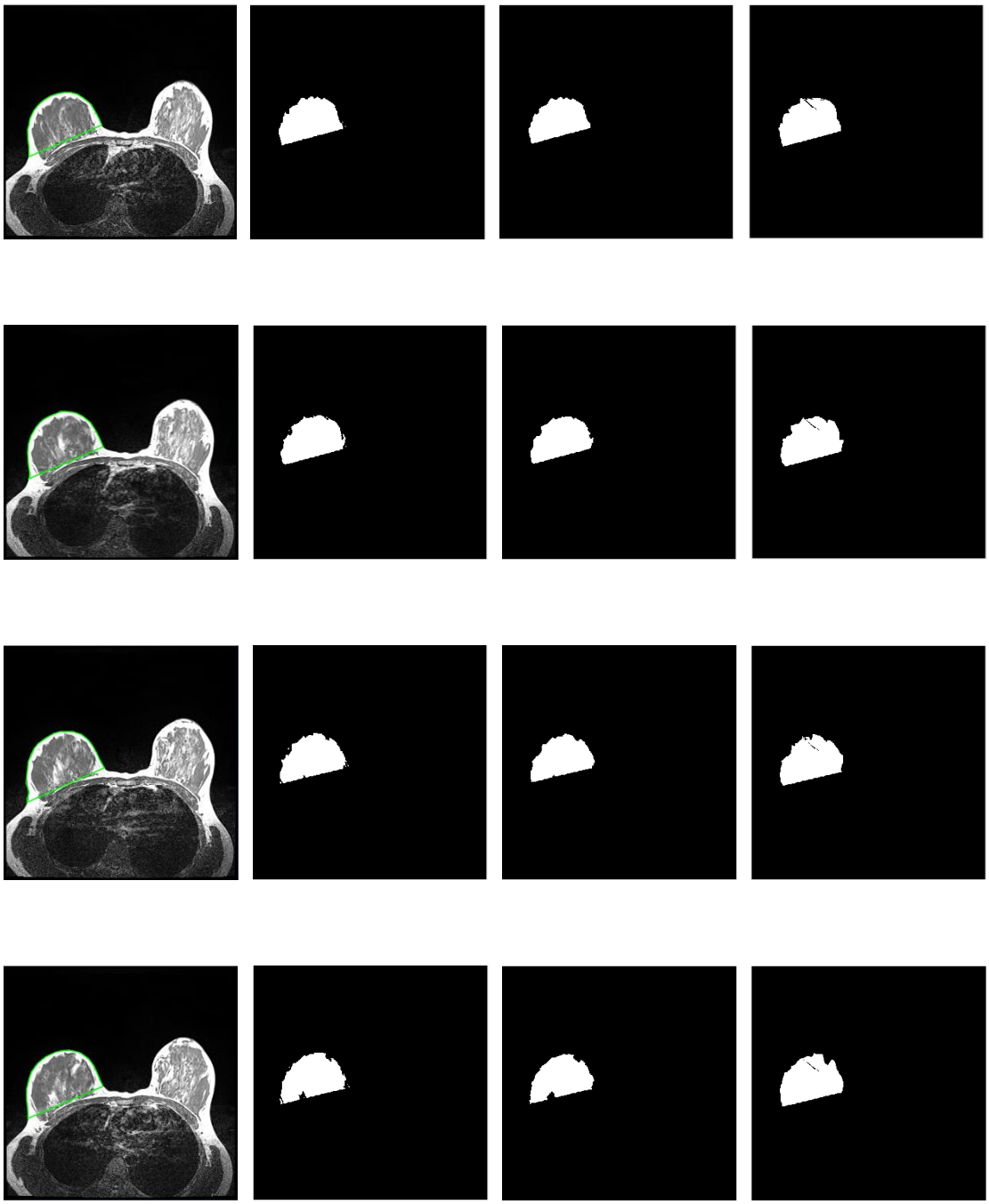

(a) (b) (c) (d)

Figure 3.16: The result of case 7 of proposed method (60 slices per case). (a) Original MRI image (green line is breast area), (b) region growing result, (c) post-processed result, (d) manual gland area by physician (Continued)

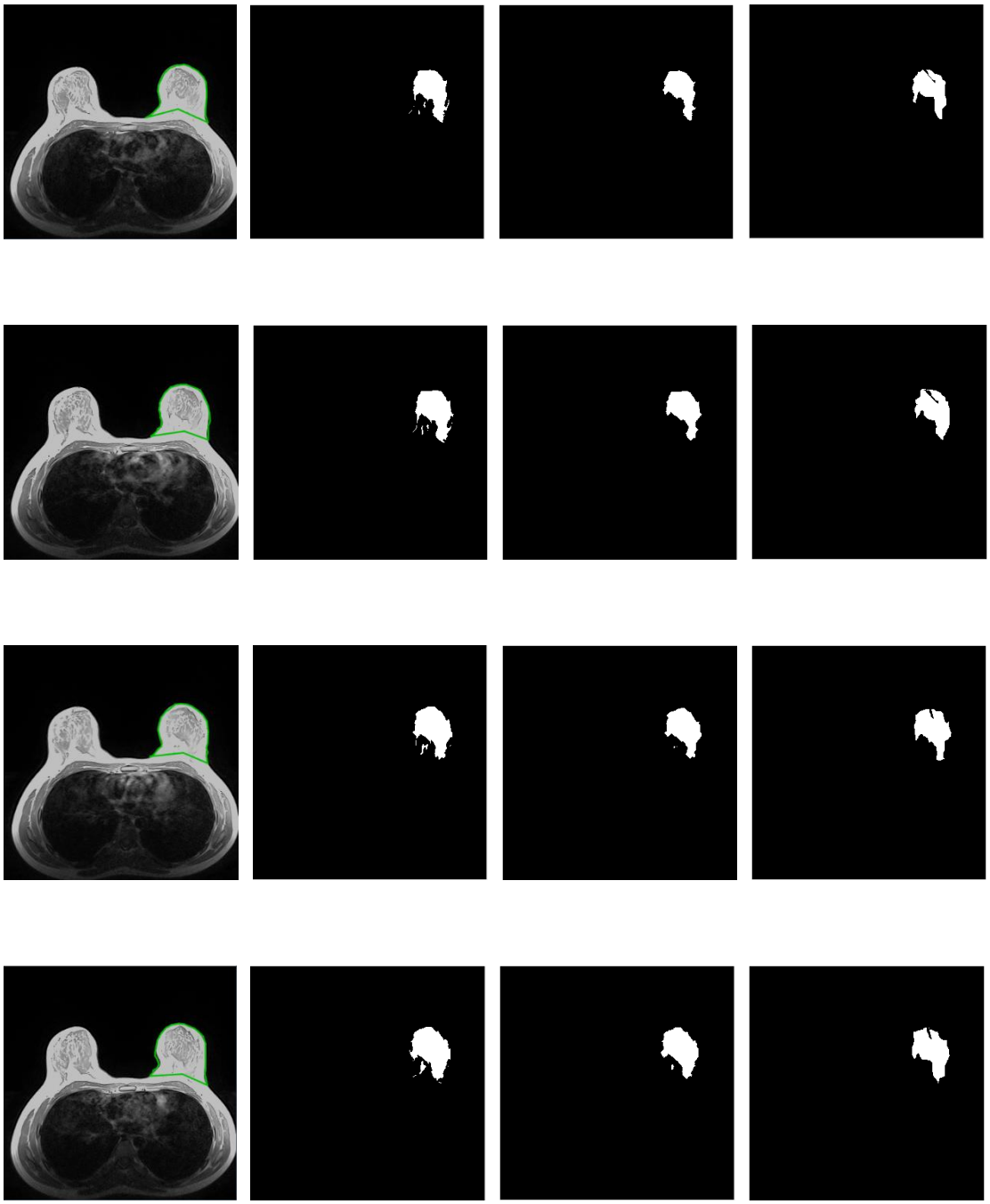

(a) (b) (c) (d)

Figure 3.17: The result of case 8 of proposed method (60 slices per case). (a) Original MRI image (green line is breast area), (b) region growing result, (c) post-processed result, (d) manual gland area by physician

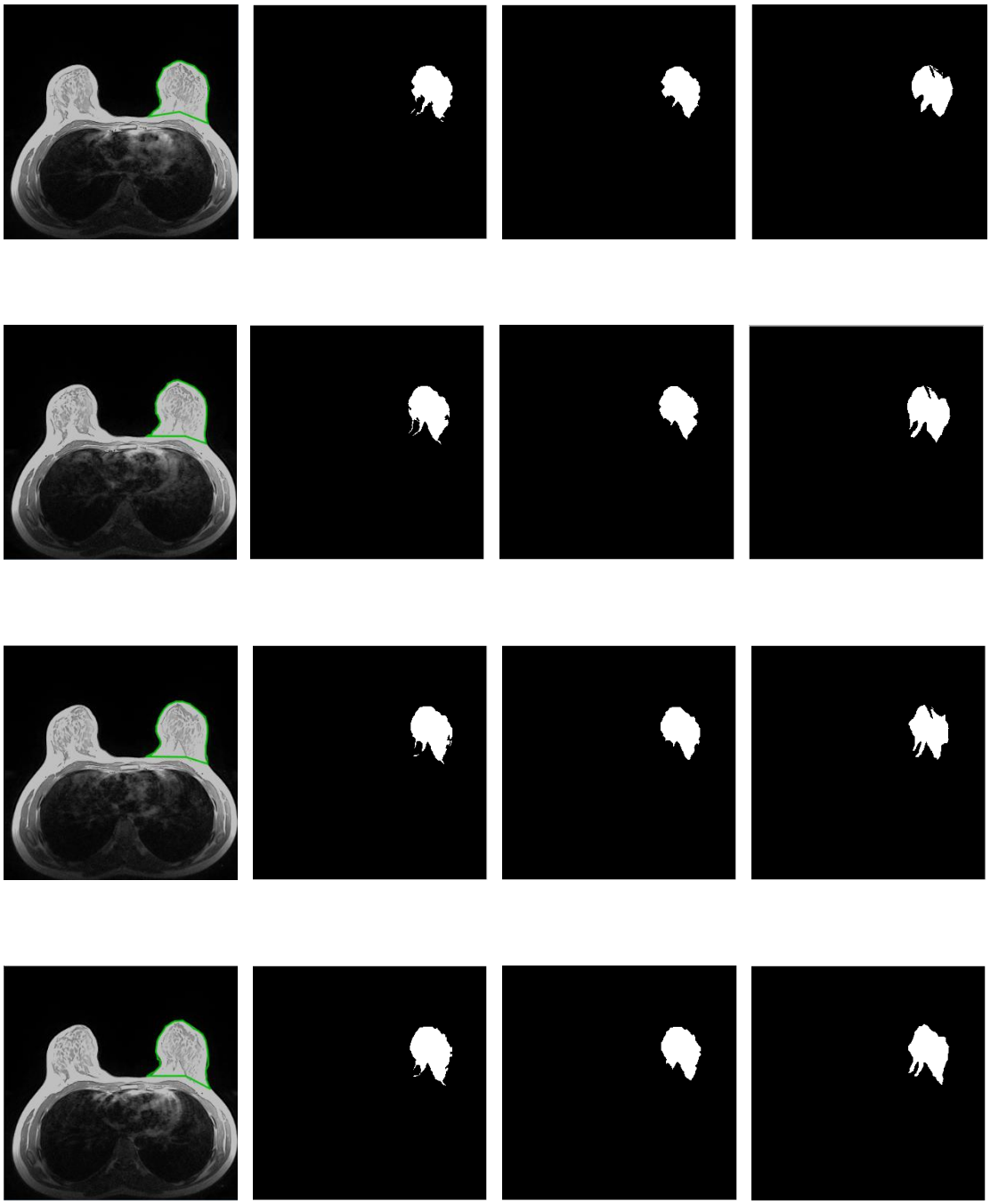

(a) (b) (c) (d)

Figure 3.17: The result of case 8 of proposed method (60 slices per case). (a) Original MRI image (green line is breast area), (b) region growing result, (c) post-processed result, (d) manual gland area by physician (Continued)

CHAPTER 4 DISCUSSION AND CONCLUSSION

The advantages of MRI are non-invasive, non-radioactive, high sensitivity and multi-view images. Therefore, breast MRI become more extensive used to diagnose breast cancer in medical imaging tools. Along with the growth of medical imaging technology, the CAD system is used in diagnosis more popularly than before. Radiologists also could acquire information that is helpful to them by CAD systems, such as the location of breast, the volume of breast, the volume of fibroglandular, breast density, even the tumor information.

This study proposed a fast and high accuracy method to identify fibroglandular tissue on breast MRI. The proposed method applied anisotropic diffusion filtering as the pre-processing step to reduce the noises and reserve the shape of the fibroglandular breast tissues. The breast area was used to locate the initial seed point and then the 3D region growing segmentation method automatically produce a precise region of the fibroglandular breast tissues. The image database including 10 cases were used to evaluation in this study. We found that the proposed method determines the breast fibroglandular region that are very similar to manual sketched region. The development of this automatic segmentation method is important and its medical application is useful. This work could reduce the wrong decision by the physician who is inexperienced.

According to the experiment of 10 cases (Table 3.1), it displays some benefits of the proposed method: (1) The proposed algorithm is adaptive to every case. User don’t need to correct any parameter. (2) It was easy to find seed points automatically. (3) User just need to select the series of MR images and the breast volume, gland volume, breast density could be computed by system. (4) It is an efficient algorithm. The calculation time for the whole segmentation of one case only take within 40

second, including pre-processing and describing the gland contour. To summarize those advantages, the result displays to be essential in computer-aided analysis systems. In addition to the segmentation result is confirmed by physicians that is precious for the breast cancer research.

The performance analysis is inspected by four practical similarity measures in Table 3.2. The SI is higher than 0.8 and the EF is lower than 0.3. It means that the proposed segmentation method is excellent and confidence. The other six cases, the breast fibroglandular area is an unconnected tissue which leads to the breast fibroglandular area drawn by the physician is incompleteness. Therefore, the similarity measures would not be applied to this cases. Moreover, when the proposed method located the center of mass which is outside the breast fibroglandular area. This situation would lead to the incorrect cutting of the regional growth method. Thus the proposed method provided a semi-automatic procedure which permitted doctor to select an appropriate seed point to segment the breast fibroglandular.

In the 10 cases of this study, the performance of a few cases was unsatisfied and then the improvements are still required. For example, the proposed system acquired an unsatisfied result of the fibroglandular region because of the insufficient gland, as shown in Fig. 4.18. In the future, we may improve our method to reach the purpose of extracting the fibroglandular tissue.

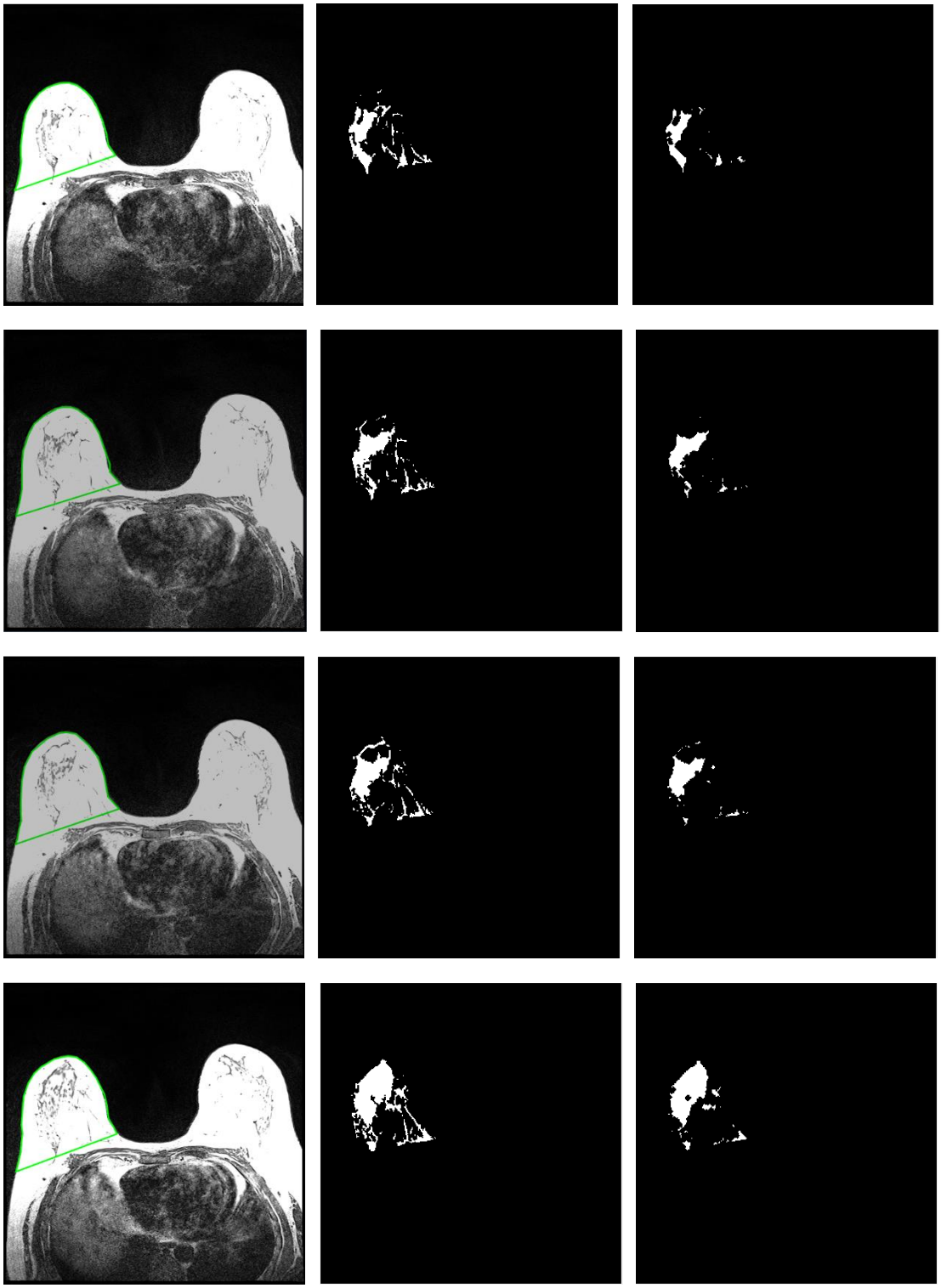

(a) (b) (c)

Figure 4.18: The defected results by the proposed method (60 slices per case). (a) Original MRI image (green line is breast area), (b) region growing result, (c) post-processed result

REFERENCES

[1] Y. C. Chang, Y. H. Huang , C. S. Huang , J. H. Chen , R. F. Chang, "Computerized breast lesions detection using kinetic and morphologic analysis for dynamic contrast-enhanced MRI," *Magnetic Resonance Imaging, vol. 32, Issue 5,* June 2014, pp. 514-522.

[2] G. Rabottino , A. Mencattini , M. Salmeri , F. Caselli , R. Lojacono, "Performance evaluation of a region growing procedure for mammographic breast lesion identification," *Computer Standards & Interfaces, vol. 33, Issue 2,*February 2011, pp. 128-135.

[3] D. H. Chen , Y. C. Chang, P. J. Huang, C. H. Wei, "The correlation cnalysis between breast density and cancer risk factor in breast MRI images," *International Symposium on Biometrics and Security Technologies (ISBAST),* September 2013, pp. 72 – 76.

[4] J. A. Rosado-Toro, T. Barr, J.-P. Galons, M. T. Marron, A. Stopeck, C. Thomson,*et al.*, "Automated segmentation of breast fat-water MR images using empirical analysis," *IEEE International Conference on Acoustics, Speech and SignalProcessing (ICASSP),* October 2013, pp. 1018-1022.

[5] S. Ribes, D. Didierlaurent, N. Decoster, E. Gonneau, L. Risser, V. Feillel, *et al.*, "Automatic segmentation of breast MR images through a markov random field statistical model," *IEEE Transactions on Medical Imaging, vol. 33,* October 2014, pp. 1986-1996.

[6] L. Wang, B. Platel, T. Ivanovskaya, M. Harz, and H. K. Hahn, "Fully automatic breast segmentation in 3D breast MRI," *IEEE International Symposium on Biomedical Imaging (ISBI),* July 2012, pp. 1024-1027.

[7] W. He, P. Hogg, A. Juette, E. R.E. Denton, R. Zwiggelaar, "Breast image

pre-processing for mammographic tissue segmentation," *Computers in Biology and Medicine, vol. 67,* December 2015, pp. 61-73.

[8] T. C. Wang, Y. H Huang, C. S. Huang, J. H. Chen, G. Y. Huang, Y. C. Chang, R.F. Chang, "Computer-aided diagnosis of breast DCE-MRI using pharmacokinetic model and 3-D morphology analysis," *Magnetic Resonance Imaging, vol. 32, Issue 3,* April 2014, pp. 197-205.

[9] A. Saha , X. Yu, D. Sahoo, M. A. Mazurowski, "Effects of MRI scanner parameters on breast cancer radiomics," *Expert Systems with Applications, vol. 87,* November 2017, pp. 384-391.

[10] R. Takahashi, Y. Kajikawa, "Computer-aided diagnosis: a survey with bibliometric Analysis," *International Journal of Medical Informatics, vol. 101,* May 2017, pp. 58-67.

[11] A. Rampun, P. J. Morrow, B. W. Scotney, J. Winder, "Fully automated breast boundary and pectoral muscle segmentation in mammograms," *Artificial Intelligence in Medicine, vol. 79,* June 2017, pp. 28-41.

[12] L. G. Shapiro and G. C. Stockman (2001): "Computer Vision," *New Jersey, Prentice-Hall, ISBN 0-13-030796-3,* pp 279-325.

[13] S. Wu, S. P. Weinstein, E. F. Conant, M. D. Schnall, and D. Kontos, "Automated chest wall line detection for whole-breast segmentation in sagittal breast MR images," *Medical physics, vol. 40,* April 2013.

[14] J. A. Martinez-Mera, P. G. Tahoces, J. M. Carreira, J. J. Suarez-Cuenca, and M. Souto, "A hybrid method based on level set and 3D region growing for

segmentation of the thoracic aorta," *Computer Aided Surgery, vol. 18,* July 2013, pp. 109-117.

[15] M. Sezgin and B. Sankur, "Survey over image thresholding techniques and quantitative performance evaluation," *Journal of Electronic Imaging, vol. 13,* January 2004, pp. 146-168.

[16] N. Otsu, "Threshold selection method from gray-level histograms," *IEEE Transactions on Systems Man and Cybernetics, vol. 9,* January 1979, pp. 62-66.

[17] J. Canny, "A computational approach to edge detection," *IEEE Trans Pattern Anal Mach Intell, vol. 8,* Jun 1986, pp. 679-698.

[18] P. Perona and J. Malik, "Scale-space and edge detection using anisotropic diffusion," *IEEE Transactions on Pattern Analysis and Machine Intelligence, vol. 12,* July 1990, pp. 629-639.

[19] A. Gumaei, A. El-Zaart, M. Hussien, and M. Berbar, "Breast segmentation using k-means algorithm with a mixture of gamma distributions," *Symposium on Broadband Networks and Fast Internet,* July 2012, pp. 97-102.

[20] M. Mustra and M. Grgic, "Robust automatic breast and pectoral muscle segmentation from scanned mammograms," *Signal processing, vol. 93,* October 2013, pp. 2817-2827.

[21] L. Wang and C. Pan, "Robust level set image segmentation via a local correntropy-based K-means clustering," *Pattern Recognition, vol. 47,* May 2014, pp. 1917-1925.

[22] R. Adams and L. Bischof, "Seeded region growing," *IEEE Transactions on Image processing, vol. 16,* June 1994, pp. 641-647.

[23] R. Rouhi, M. Jafari, S. Kasaei, and P. Keshavarzian, "Benign and malignant breast tumors classification based on region growing and CNN segmentation," *Expert Systems with Applications, vol. 42,* February 2015, pp. 990-1002.

[24] A. Gubern-MC rida, M. Kallenberg, R. M. Mann, R. Marti, and N. Karssemeijer,"Breast segmentation and density estimation in breast MRI: a fully automatic framework," *IEEE Journal of Biomedical and Health Informatics, vol. 19,* January 2015, pp. 349-357.

[25] T. Y. Liu, Y. L. Huang, and D. R. Chen, "Precise Three-Dimensional segmentation for breast region on MRI," *International Conference on Engineering & Technology, Computer, Basic & Applied Sciences, on Taipei, Taiwan,* June 2016.

[26] R. C. Gonzalez and R. E. Woods, "Digital Image Processing 3nd Edition," *Chapter 10.3 Thresholding,* 2008, pp. 738-763.

[27] A. Mehnert and P. Jackway, "An improved seeded region growing algorithm," *Pattern Recognition Letters, vol. 18,* October 1997, pp. 1065-1071.

[28] R. C. Gonzalez and R. E. Woods, "Digital Image Processing 3nd Edition," *Chapter 10.4 Region Growing Segmentation,* 2008, pp. 763-769.

[29] R. C. Gonzalez and R. E. Woods, "Digital Image Processing 3nd Edition," *Chapter 9 Morphological Image Processing,* 2008, pp. 628-642.

[30] HOLOGIC, "Understanding Quantra™ 2.0 User Manual," *MAN-02004 Rev 004*.